THE JOURNAL OF BIOLOGICAL CHEMISTRY
Vol. 279, No. 45, Issue of November 5, pp. 46962–46968, 2004

Printed in U.S.A.

PSD-95 and Lin-7b Interact with Acid-sensing Ion Channel-3 and Have Opposite Effects on H^+-gated Current*

Received for publication, May 26, 2004, and in revised form, August 13, 2004
Published, JBC Papers in Press, August 17, 2004, DOI 10.1074/jbc.M405874200

Alesia M. Hruska-Hageman‡§¶, Christopher J. Benson‡, A. Soren Leonard‡§, Margaret P. Price‡, and Michael J. Welsh‡§‖**

From the Departments of ‡Internal Medicine and ‖Physiology and Biophysics and the §Howard Hughes Medical Institute, Roy J. and Lucille A. Carver College of Medicine, University of Iowa, Iowa City, Iowa 52242

The acid-sensing ion channel-3 (ASIC3) is a degenerin/epithelial sodium channel expressed in the peripheral nervous system. Previous studies indicate that it participates in the response to mechanical and painful stimuli, perhaps contributing to mechanoreceptor and/or H^+-gated nociceptor function. ASIC3 subunits contain intracellular N and C termini that may control channel localization and function. We found that a PDZ-binding motif at the ASIC3 C terminus interacts with four different proteins that contain PDZ domains: PSD-95, Lin-7b, MAGI-1b, and PIST. ASIC3 and these interacting proteins were expressed in dorsal root ganglia and spinal cord, and PSD-95 co-precipitated ASIC3 from spinal cord. When expressed in heterologous cells, PSD-95 reduced the amplitude of ASIC3 acid-evoked currents, whereas Lin-7b increased current amplitude. PSD-95 and Lin-7b altered current density by decreasing or increasing, respectively, the amount of ASIC3 on the cell surface. The finding that multiple PDZ-containing proteins bind ASIC3 and can influence its presence in the plasma membrane suggests that they may play an important role in the contribution of ASIC3 to nociception and mechanosensation.

ASIC3[1] is a non-voltage-gated Na^+ channel activated by acidic extracellular solutions (1, 2). It is expressed in the peripheral nervous system, including the dorsal root ganglia and trigeminal ganglia. Immunocytochemical studies have localized it to several different specialized sensory nerve endings of skin, suggesting it might participate in mechanosensation and nociception (3). The importance of ASIC3 for sensory function was revealed by studies of mice bearing targeted disruptions of the *ASIC3* gene (3, 4). In single fiber recordings from cutaneous nerves, loss of ASIC3 increased the sensitivity of mechanoreceptors detecting light touch but reduced the sensitivity of a mechanoreceptor responding to noxious pinch. In behavioral studies, ASIC3 modulated the response to noxious acid, heat, and mechanical stimuli. Moreover chronic mechanical hyperalgesia produced by intramuscular acid injections was prevented in ASIC3 null animals (5). Functional studies suggest that ASIC3 may also mediate the pain associated with myocardial ischemia (6, 7). Thus, in different cellular contexts, ASIC3 may participate in the responses to both mechanical and acidotic stimuli to mediate normal touch and pain sensation.

ASIC3, a member of the DEG/ENaC family, forms heteromultimers in neurons with other DEG/ENaC subunits, ASIC1 and ASIC2, to generate H^+-gated cation channels (8–10). ASIC3 shares the overall structure of DEG/ENaC proteins, including two transmembrane domains, a large extracellular loop containing 14 conserved cysteines, and intracellular N and C termini (11, 12). The intracellular domains of ASIC subunits might have several functions, including localizing the channels, controlling the number of channels on the cell surface, regulating channel function, and forming part of a scaffold important for the response to mechanical stimuli (11–13). Two proteins have been shown to interact with the intracellular domains of ASIC channels. The C termini of ASIC1 and ASIC2 share homology with type II PDZ (PSD-95, *Drosophila* discs-large protein, zonula occludens protein-1)-binding domains and bind PICK1 (protein interacting with C kinase-1) (14, 15). PICK1 may facilitate the interaction of ASIC2a with protein kinase C, and the interaction between ASIC1 and PICK1, regulated by phosphorylation, may provide a mechanism to control the cellular localization of ASIC1 (16, 17). The ASIC3 C terminus shares homology with type I PDZ-binding motifs. CIPP (channel-interacting PDZ domain protein), which contains four PDZ domains, is reported to interact with the ASIC3 C terminus and increase H^+-gated current (18).

The potential importance of protein-protein interactions for ASIC3 function led us to ask what proteins bind its intracellular domains. To identify interacting proteins, we used the yeast two-hybrid system and a candidate gene approach.

EXPERIMENTAL PROCEDURES

Yeast Two-hybrid Assay—Construction of the bait plasmid, hASIC3 (residues 476–531), in the GAL4(DB) vector pAS2-1 (Clontech) was described previously (14). This bait construct was transformed into the PJ692A yeast strain using the lithium acetate procedure and mated with yeast strain Y187 pretransformed with the human brain Matchmaker cDNA library (Clontech). The mRNA source was a normal, whole brain from a 37-year old Caucasian male as reported on the Clontech product analysis certificate. Mated cells were plated on Leu^-/Trp^-/His^-

* Work done in the *In Vitro* Models and Cell Culture Core was supported by the NHLBI, National Institutes of Health; by Cystic Fibrosis Foundation Grants R458-CR02 and ENGLH9850; and by NIDDK, National Institutes of Health Grant DK54759. The costs of publication of this article were defrayed in part by the payment of page charges. This article must therefore be hereby marked "*advertisement*" in accordance with 18 U.S.C. Section 1734 solely to indicate this fact.

¶ An associate of the Howard Hughes Medical Institute.

** An investigator of the Howard Hughes Medical Institute. To whom correspondence should be addressed: Howard Hughes Medical Inst., Roy J. and Lucille A. Carver College of Medicine, 500 EMRB, University of Iowa, Iowa City, IA 52242. Tel.: 319-335-7619; Fax: 319-335-7623; E-mail: michael-welsh@uiowa.edu.

[1] The abbreviations used are: ASIC, acid-sensing ion channel; DEG/ENaC, degenerin/epithelial sodium channel; PDZ, PSD-95, *Drosophila* discs-large protein, zonula occludens protein-1; PSD-95, postsynaptic density-95 protein; PICK1, protein interacting with C kinase-1; CIPP, channel-interacting PDZ domain protein; MAGI, membrane-associated guanylate kinase with inverted orientation; PIST, PDZ protein interacting specifically with TC10; NR2, *N*-methyl-D-aspartate receptor subunit 2; RT, reverse transcription; DRG, dorsal root ganglion; GFP, green fluorescent protein; HA, hemagglutinin; CHO, Chinese hamster ovary; MES, 4-morpholineethanesulfonic acid; CAL, CFTR-associated ligand; CFTR, cystic fibrosis transmembrane conductance regulator.

plates supplemented with 5 mM 3-amino-1,2,4-triazole and grown for 10 days at 30 °C before positive clones were picked and streaked on plates lacking adenine, His, Leu, and Trp. Library plasmids from clones that grew in the absence of adenine, His, Leu, and Trp and that tested positive for β-galactosidase expression were isolated. They were co-transformed with either the bait vector or the original pAS2-1 vector into PJ69-2A to confirm the interaction. Those that were specific for the bait were sequenced.

DNA Constructs—hASIC3 (residues 476–531), hASIC1 (residues 459–528), hASIC2 (residues 470–512), hαENaC (residues 589–669), and hβENaC (residues 559–640) in the GAL4(DB) vector pAS2-1 and the full-length mASIC3 construct in pMT3 were described previously (14). The hASIC3 deletion constructs used for the yeast two-hybrid experiments were made by using the QuikChange site-directed mutagenesis kit (Stratagene, La Jolla, CA) for residues 476–527 and subcloning using PCR to amplify and insert the C-terminal deletions of hASIC3 residues 476–523, 476–513, and 513–531 into the unique EcoRI and BamHI sites of the GAL(DB) vector. Point mutations in the C terminus of the hASIC3 (residues 476–531) in pAS2-1 (see Fig. 1*C*) were made using the QuikChange site-directed mutagenesis kit. The mASIC3Δ4 (mASIC3 minus the C-terminal 4 amino acids) construct in pMT3 was also made using the QuikChange mutagenesis kit. The GFP-tagged rat PSD-95 construct was a gift from David Bredt, the Myc-tagged mouse Lin-7b construct was a gift from Ben Margolis, the FLAG-tagged mouse MAGI-1b used in the coimmunoprecipitation experiments was a gift from Irina Dobrosotskaya, the Myc-tagged PSD-95 construct was a gift from Johannes Hell, and the HA-tagged mouse PIST (PDZ protein interacting specifically with TC10) was a gift from Ian Macara. The rat ASIC3 cDNA (used in the electrophysiology studies) was cloned by reverse transcription (RT)-PCR of RNA isolated from Sprague-Dawley rat dorsal root ganglia using the 5′ primer 5′-CCA TCG ATG GAG CCA TGA AAC CTC GCT CCG GAC TGG AGG AGG CCC AG-3′ and the 3′ primer 5′-TCC CAC CGT ACC TGT TAC CTC GTC ACA AGG CTC TAG GGG GTA CCC C-3′. Mouse ASIC1a was cloned as described previously (10). The rat ASIC3Δ4 construct (rASIC3 minus the C-terminal 4 amino acids) and the mouse ASIC1vtrl construct in which the residues VTRL were substituted for the last 4 amino acids of ASIC1a were generated using the QuikChange site-directed mutagenesis kit (Stratagene) and were cloned into pMT3 for expression in CHO cells. All plasmid constructs were confirmed by DNA sequencing.

Antibodies—Anti-mASIC3 (anti-DRASIC) and anti-hASIC1 (anti-hASIC) were described previously (3, 14, 19), guinea pig anti-ASIC3 was purchased from Chemicon (Temecula, CA), anti-PSD-95 and anti-Lin-7 were purchased from Sigma, anti-HA was purchased from Roche Applied Science, anti-MAGI-1 (sc-11523) was purchased from Santa Cruz Biotechnology, Inc. (Santa Cruz, CA), and mouse monoclonal anti-Myc (clone 9E10) was from the Developmental Studies Hybridoma Bank (Iowa City, IA).

COS-7 and CHO Cell Culture and Transfection—COS-7 cells were maintained in culture with Dulbecco's modified Eagle's medium plus 10% fetal calf serum in a humidified atmosphere of 5% CO_2 in air at 37 °C. COS-7 cells were transfected by electroporation using 10^7 cells with 20–30 μg of plasmid DNA at a 1:1 ratio (ASIC construct or empty vector:interacting protein construct or empty vector). CHO cells were cultured in F12 medium with 10% fetal bovine serum and 1% penicillin/streptomycin at 37 °C. CHO cells were transfected with cDNAs using cationic lipid (TransFast, Promega) following the manufacturer's recommendations. ASIC subunits (0.18 μg/1.5 ml) and PDZ proteins (or dsRed as a control cDNA) (1.82 μg/1.5 ml) were cotransfected at a 1:10 ratio. cDNA for green fluorescent protein (0.33 μg/1.5 ml) was also expressed to facilitate detection of transfected cells by epifluorescence. We have found that >90% of green cells generated ASIC-like current and <5% of non-green cells have acid-activated current. CHO cells were studied 48–72 h after transfection.

Immunoprecipitation from COS-7 Cells—Transfected cells were lysed 48 h post-transfection at 4 °C in lysis buffer (50 mM Tris, pH 7.4, 150 mM NaCl, 1% Triton X-100, 0.4 mM phenylmethylsulfonyl fluoride, 20 μg/ml aprotinin, 20 μg/ml leupeptin, 10 μg/ml pepstatin A) for PSD-95-GFP and (20 mM Tris, pH 7.4, 100 mM NaCl, 1 mM EDTA, pH 8, 1% Triton X-100, 0.4 mM phenylmethylsulfonyl fluoride, 20 μg/ml aprotinin, 20 μg/ml leupeptin, 10 μg/ml pepstatin A) for FLAG-MAGI-1b, Myc-Lin-7b, and HA-PIST as described previously (20). We used 5% of the lysate for Western blot, and the remainder was incubated with the indicated antibody overnight at 4 °C. Proteins were separated on 8% (10% for Myc-Lin-7b) SDS-polyacrylamide gels. Western blots were blocked with 5% bovine serum albumin and incubated first with primary antibody (anti-mASIC3 serum (1:5000), anti-hASIC serum (1:5000), anti-PSD-95 (1:15,000), anti-MAGI-1 (1:250), anti-Lin-7 (1:2500), or anti-HA (1:7500)) and then with either a horseradish peroxidase-coupled secondary antibody (1:5000) (Amersham Biosciences) or horseradish peroxidase-linked Protein A (1:10,000) (Amersham Biosciences). Proteins were detected by enhanced chemiluminescence (Pierce).

Immunoflourescence—COS-7 cells were grown on chamber slides coated with collagen. Cells were fixed with 4% formaldehyde in phosphate-buffered saline, permeabilized with 0.1% Triton X-100 in phosphate-buffered saline, blocked with SuperBlock (Pierce), and incubated with primary antibodies anti-mASIC3 serum (1:750) and anti-PSD-95 (1:8000), anti-Myc (1:1000), or anti-HA (1:250); guinea pig anti-ASIC3 (1:600) and anti-Myc (1:1000) followed by the secondary antibodies goat anti-rabbit Alexa 568 (1:1250) and goat anti-mouse Alexa 488 (1:1250); or goat anti-guinea pig Alexa 568 (1:1250) and goat anti-mouse Alexa 488 (1:1250) (Molecular Probes, Eugene, OR). Staining was visualized using a confocal microscope (Bio-Rad 1024).

RT-PCR—For RT-PCR analysis, first strand cDNA was synthesized with Superscript II (Invitrogen) with random hexamer primers using mouse brain, spinal cord, and dorsal root ganglion RNA. The following primers were used for PCR amplification: MAGI-1b, 5′-ATGATCCCTCC-TAAAATCGCT-3′ and 5′-CTTCCGGAACTCCTTGTGCAC-3′ (138-bp band); PIST, 5′-GGACAGCCTGCGGATAGATGT-3′ and 5′-ACGATAGC-GGTGTCCACTCTC-3′ (215-bp band); Lin-7b, 5′-AGCGGAGAGCTGCC-CCCGCAG-3′ and 5′-ATGAGCCCGCACCTCGGCGCT-3′ (139-bp band); ASIC3, 5′-GGGGAGTTCCACCATAAGACCACC-3′ and 5′-CTTCCAGA-TGGGCAGATACTCCTC-3′ (450-bp band); PSD-95, 5′-TCAGGTCTGGG-CTTCAGCATC-3′ and 5′-CCGGCGCATGACGTAGAGGCG-3′ (113-bp band). The cycling parameters using the RoboCycler thermocycler (Stratagene) consisted of 40 cycles of 94 °C for 45 s, 60 °C for 45 s, and 72 °C for 2 min.

Immunoprecipitation from Tissue—Rat tissues (brain, spinal cord, and dorsal root ganglia) were isolated and frozen at −80 °C. Lysates were made from the frozen tissue as described previously (21). PSD-95, ASIC3, or ASIC1 was precipitated by adding anti-PSD-95, anti-mASIC3 (3), or anti-hASIC 6.4 affinity-purified antibodies (19) to 500 μg of tissue extracts in a final buffer of 25 mM HEPES, pH 7.4, 100 mM NaCl, 5 mM EGTA, 5 mM EDTA, 1% deoxycholate, 1 mM β-mercaptoethanol, 0.4 mM phenylmethylsulfonyl fluoride, 20 μg/ml aprotinin, 20 μg/ml leupeptin, 10 μg/ml pepstatin A and rocking at 4 °C. Protein A-Sepharose (Pierce) (3–5 mg, preswollen and washed three times with TBS (10 mM Tris-Cl, pH 7.4, 150 mM NaCl) was added to the samples and mixed for 2.5 h. The immunocomplexes were sedimented by centrifugation and washed three times with 1% Triton X-100 in TBS and once with 10 mM Tris-Cl, pH 7.4, before being extracted with 20 μl of SDS sample buffer (2% SDS, 20 mM dithiothreitol, 10% sucrose, 125 mM Tris-Cl, pH 6.8) for 20 min at 60 °C.

Proteins were separated by SDS-PAGE, transferred to nitrocellulose, blocked with 3% bovine serum albumin in TBS (TBS-bovine serum albumin) and incubated with anti-PSD-95 (1:1000), anti-mASIC3 (1:250), or anti-hASIC 6.4 (1:1000) affinity-purified antibody for 2 h. The blots were washed five times with TBS-bovine serum albumin, incubated with horseradish-peroxidase-labeled protein A (1:10,000), washed with 0.05% Tween 20 in TBS, and developed with the enhanced chemiluminescence reagent (Pierce).

Electrophysiology—Whole-cell patch clamp recordings (at −70 mV) from CHO cells were performed with an Axopatch 200B amplifier (Axon Instruments, Foster City, CA) and acquired and analyzed with Pulse/Pulsefit 8.30 (HEKA Electronics, Lambrecht, Germany) and Igor Pro 3.16 (WaveMetrics, Lake Oswego, OR) software. Experiments were performed at room temperature. Currents were filtered at 5 kHz and sampled at 2 or 0.2 kHz. Series resistance was compensated by at least 50%. Micropipettes (2–5 megaohms) were filled with internal solution: 100 mM KCl, 10 mM EGTA, 40 mM HEPES, and 5 mM $MgCl_2$, pH 7.4 with KOH. External solution contained: 120 mM NaCl, 5 mM KCl, 1 mM $MgCl_2$, 2 mM $CaCl_2$, 10 mM HEPES, 10 mM MES, pH adjusted with tetramethylammonium hydroxide, and osmolarity adjusted with tetramethylammonium chloride. Extracellular solutions were changed within 20 ms using a computer-driven solenoid valve system (10). Data are means ± S.E. Kinetics of desensitization were fit with single exponential equations, and time constants (τ) are reported. Statistical differences were assessed by two-tailed Student's *t* test.

Surface Biotinylation—Surface proteins on 48-h post-transfected COS-7 cells were labeled with cell-impermeable EZ-Link sulfo-*N*-hydroxysuccinimidobiotin (Pierce), 0.25 mg/ml in phosphate-buffered saline, at 4 °C for 20 min following the manufacturer's recommendations. After labeling, cells were washed two times with TBS and lysed in lysis buffer (25 mM HEPES, pH 7.4, 100 mM NaCl, 5 mM EGTA, 5 mM EDTA, 1% Triton X-100, 0.5% sodium deoxycholate, 1% SDS, 0.4 mM phenylmethylsulfonyl fluoride, 20 μg/ml aprotinin, 20 μg/ml leupeptin, 10 μg/ml pepstatin A). Cell surface proteins were isolated by incubating

500 μg of the lysate with immobilized neutravidin beads (Pierce) at 4 °C for 2 h. Total ASIC3 protein was isolated by incubating 500 μg of the same lysate as above with anti-mASIC3 antibodies at 4 °C for 2 h followed by incubation with protein A-Sepharose (prewashed as above). The bound proteins were eluted with sample buffer (2% SDS, 20 mM dithiothreitol, 10% sucrose, 125 mM Tris-Cl, pH 6.8) for 20 min at 65 °C, subjected to SDS-PAGE, Western blotted with anti-mASIC3 antibodies, and developed with the enhanced chemiluminescence reagent (Pierce). We used 10 μg of the total lysate for Western blotting.

RESULTS

Identification of MAGI-1b, Lin-7b, and PIST with a Yeast Two-hybrid Screen—To find proteins that interact with ASIC3, we used its intracellular C terminus as the bait to screen a human brain cDNA library in the yeast two-hybrid system. We identified three clones specific for the bait: MAGI-1b (amino acids 642–1287), Lin-7b (amino acids 40–207), and PIST (amino acids 46–462). Each clone was missing sequence that encoded the N-terminal portion of the protein but included the C-terminal end. All three clones encoded at least one PDZ domain.

MAGI-1b is a membrane-associated guanylate kinase that contains two WW domains, a guanylate kinase domain, and five PDZ domains (22). The clone we identified contained PDZ domains 2–5. MAGI-1b is a member of a family of MAGI proteins, and several different splice variants of MAGI-1 have been identified including MAGI-1a, -1b, and -1c (22, 23).

Lin-7b, also named MALS (mammalian Lin-7 protein) or Veli (vertebrate LIN-7 homologs) contains an N-terminal domain that binds CASK and a PDZ domain at its C terminus (24–26). Both Lin-7b and MAGI isoforms are thought to provide a scaffold linking receptors and channels with cytoskeletal proteins and enzymes at sites of cell-cell contact such as tight junctions in epithelial cells and synapses in neurons.

PIST is an intracellular protein first identified by its interaction with TC10, a Rho GTPase (27). PIST contains two coiled-coil domains, a leucine zipper domain embedded in the second coiled-coil domain, and a PDZ domain at its C terminus. Splice variants of PIST, such as CAL (CFTR-associated ligand) and FIG (fused in glioblastoma), are thought to participate in the trafficking of proteins out of the trans-Golgi network and retention of membrane proteins inside the cell (28, 29).

The interaction of MAGI-1b, Lin-7b, and PIST was specific for the ASIC3 C terminus; the C termini of ASIC1, ASIC2, αENaC, and βENaC failed to interact with these proteins (Fig. 1*A*). Deleting the distal half of the ASIC3 C terminus eliminated the interaction with all three proteins, whereas eliminating the N-terminal half had no effect (Fig. 1*B*). Moreover deleting the last 4 or 8 C-terminal residues also abolished the interaction.

These results suggested that ASIC3 interacts with the three PDZ domain proteins via a PDZ-binding motif at its C terminus. The C-terminal 4 residues of hASIC3 (VTQL) correspond to a type I PDZ-binding motif (*X*(S/T)*X*(V/L/I) where *X* is any amino acid) (30). Mutating the Leu at the 0 position to Ala abolished the interaction with MAGI-1b, Lin-7b, and PIST (Fig. 1*C*). In addition, mutating the Thr at the −2 position abolished the interaction with MAGI-1b and Lin-7b (PIST was not tested). In contrast, mutating the −3 Val had no effect on the interactions. Mutation of the −1 Gln did not alter the interaction with MAGI-1b or Lin-7b but disrupted the interaction with PIST. Thus, binding conforms to an interaction between the ASIC3 C terminus and PDZ domains in MAGI-1b, Lin-7b, and PIST most likely through their PDZ domains.

ASIC3 Interacts with MAGI-1b, Lin-7b, and PIST in COS-7 Cells—To test the interaction between ASIC3 and these proteins, we transfected COS-7 cells with mouse ASIC3 and epitope-tagged MAGI-1b, Lin-7b, and PIST. Immunoprecipitating ASIC3 co-precipitated each of these PDZ proteins (Fig. 2). We used PIST to test the importance of the C-terminal 4 residues in the interaction with PDZ domain-containing proteins. Deleting the last 4 residues of ASIC3 (ASIC3Δ4) prevented co-precipitation of PIST.

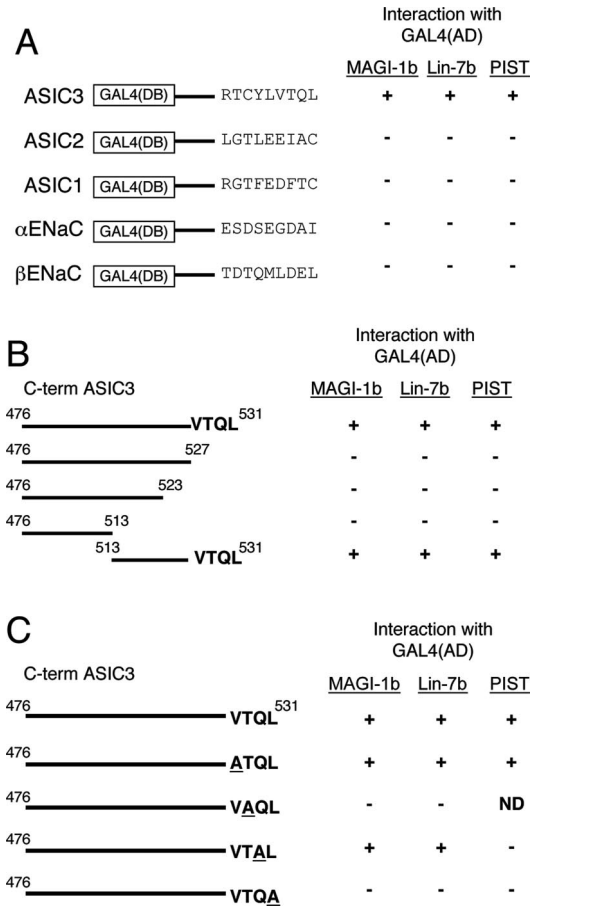

FIG. 1. **MAGI-1b, Lin-7b, and PIST interact specifically with the C terminus of ASIC3 in the yeast two-hybrid system.** *A*, the intracellular C-terminal regions of ASIC1, ASIC2, ASIC3, αENaC, and βENaC were fused to the GAL4(DB) and tested for interaction with MAGI-1b, Lin-7b, and PIST in the yeast two-hybrid system. *B*, the ASIC3 C terminus (*C-term*) containing the indicated deletions was tested for interaction with MAGI-1b, Lin-7b, and PIST. *C*, the ASIC3 C terminus containing the indicated mutations to Ala was tested for interactions. "+" indicates an interaction, "−" indicates the lack of interaction, and "*ND*" indicates not determined.

PSD-95 Interacts with ASIC3 and Requires Its PDZ-binding Domain—In addition to their interaction with ASIC3, previous studies showed that the PDZ domain-containing proteins MAGI-2 (the major neuronal MAGI protein) and Lin-7 interact with the *N*-methyl-D-aspartate receptor subunits (26, 31). Previous studies showed that the PDZ domain scaffolding protein PSD-95 also interacts with NR2 subunits (32). PSD-95 contains a Src homology 3 domain, a guanylate kinase domain, and three N-terminal PDZ domains (33). In addition, both MAGI-2 and PSD-95 interacted with shaker type K^+ channels and the neuronal cell surface molecule neuroligin (31, 34, 35). Therefore, we hypothesized that ASIC3 may bind PSD-95 via its PDZ-binding domain. Supporting this hypothesis, we found that ASIC3 co-immunoprecipitated PSD-95, and PSD-95 co-precipitated ASIC3 in COS-7 cells (Fig. 3, *A* and *B*). As controls, neither ASIC1a nor ASIC3 missing its C-terminal 4 residues co-precipitated PSD-95 (Fig. 3*C*). These data suggest that ASIC3 interacts with PSD-95 through its PDZ-binding motif.

Coexpressing ASIC3 Alters the Cellular Distribution of PSD-95 and PIST—Previous studies have shown that coexpressing a

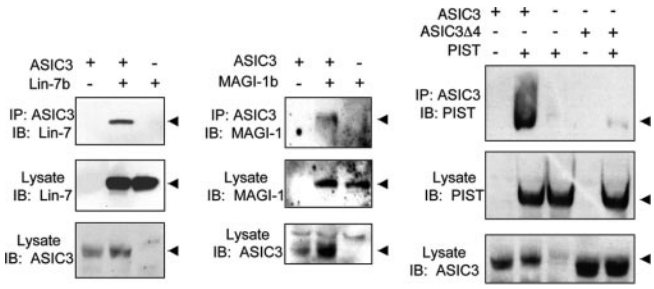

FIG. 2. **ASIC3 interacts with MAGI-1b, Lin-7b, and PIST in COS-7 cells.** COS-7 cells were transfected with expression vectors encoding full-length FLAG-MAGI-1b, Myc-Lin-7b, or HA-PIST alone or with ASIC3 or ASIC3Δ4, then immunoprecipitated (*IP*) with anti-ASIC3 antibodies, and immunoblotted (*IB*) for the indicated protein. Total lysates from the same samples were resolved by SDS-PAGE and probed with appropriate antibodies to confirm expression.

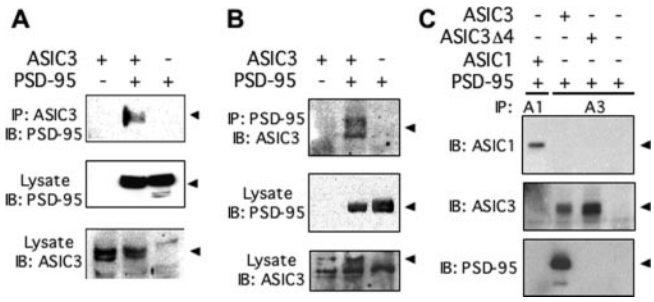

FIG. 3. **PSD-95 interacts with ASIC3 in COS-7 cells through its PDZ-binding domain.** COS-7 cells were transfected with expression vectors encoding full-length PSD-95-GFP alone or with ASIC3. *A*, immunoprecipitation (*IP*) with anti-ASIC3 antibody and immunoblot (*IB*) with anti-PSD-95 antibody. *B*, immunoprecipitation with anti-PSD-95 antibody and blot with anti-ASIC3 antibody. *C*, cotransfection with PSD-95-GFP and ASIC3, ASIC3Δ4, or ASIC1a followed by the indicated precipitations and blots. *A1*, ASIC1; *A3*, ASIC3.

PDZ domain protein and its interacting partner in some cases alters the cellular distribution of one or both proteins. The distribution often assumes a clustered pattern with protein-protein binding at intracellular sites. This appearance indicates an interaction between the two proteins but does not necessarily indicate an altered distribution at the cell surface. For example, PSD-95 expression caused clustering of shaker type K^+ channels (34), and MAGI-2 clustered the *N*-methyl-D-aspartate receptor NR2A in transfected COS-7 cells (36). To determine whether Lin-7b, PIST, MAGI-1b, or PSD-95 alters ASIC3 distribution, we expressed these proteins in COS-7 cells. When expressed alone, all four PDZ domain-containing proteins showed a diffuse staining pattern throughout the cell, whereas ASIC3 showed a reticular pattern (Fig. 4*A*). Coexpressing ASIC3 and PSD-95 altered the distribution of both proteins so that they colocalized in small clusters (Fig. 4*B*). In addition, coexpressing ASIC3 changed the distribution of PIST so that it overlapped the reticular expression pattern of ASIC3. In contrast, neither ASIC3 nor Lin-7b (Fig. 4*B*) or MAGI-1b (not shown) changed their distribution when coexpressed. Deleting 4 residues from the ASIC3 C terminus prevented the co-localization of ASIC3 and PSD-95 and prevented the redistribution of PIST (Fig. 4*B*). Taken together, the yeast two-hybrid data, the co-immunoprecipitation results, and the colocalization indicate that the ASIC3 PDZ-binding motif interacts with the PDZ domains of PSD-95, Lin-7b, PIST, and MAGI-1b. However, the colocalization results also suggested the potential for different functional consequences when the proteins interact.

ASIC3 and Interacting Proteins Are Expressed in Spinal Cord and DRG—Expression of Lin-7b, PSD-95, MAGI-1b and PIST has been reported in the central nervous system (22, 24–27, 33), whereas ASIC3 expression has been described primarily in peripheral neurons (1–3). To test whether expression occurs in the same tissue, we used RT-PCR to detect their transcripts. We found Lin-7b, PSD-95, MAGI-1b, and PIST mRNA present in DRG, spinal cord, and brain (Fig. 5). ASIC3 transcripts were also detected in all three tissues.

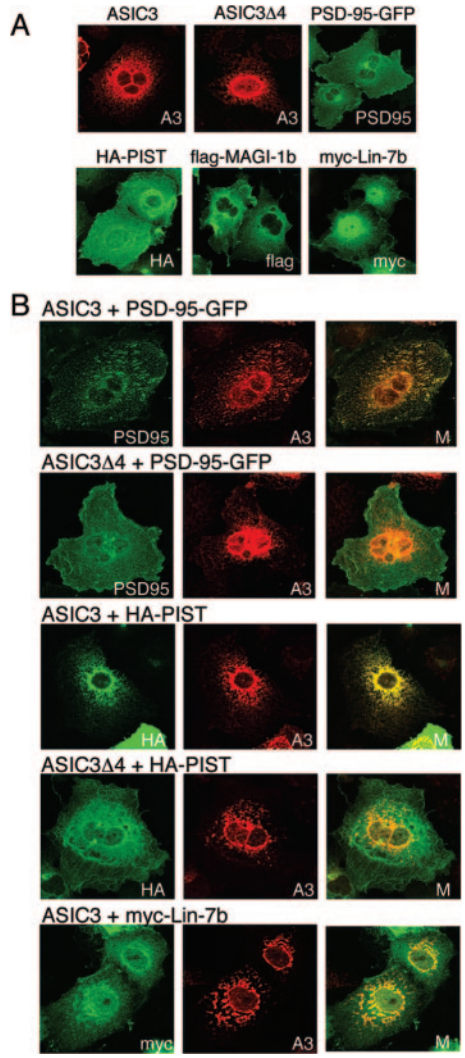

FIG. 4. **Immunostaining of ASIC3, ASIC3Δ4, PSD-95, PIST, MAGI-1b, and Lin-7b.** COS-7 cells were transfected with the indicated constructs. *A*, expression of individual constructs. *B*, coexpression as indicated with anti-ASIC3 in *red* and other proteins in *green*. Merged (*M*) images are on the *right*. *A3*, ASIC3.

Although we detected PSD-95 transcripts in DRG, previous studies reported PSD-95 in brain and spinal cord but not DRG (37). To test for PSD-95 in the DRG, we immunoprecipitated and blotted for the protein. As previously described, we found the protein in brain and spinal cord (Fig. 6*A*). Although in lower abundance, we also detected PSD-95 in the DRG. Likewise we asked whether ASIC3 protein was present outside the peripheral nervous system and found it in the spinal cord (Fig. 6*B*). Although the ability of commercially available antibodies to detect the other PDZ domain proteins limited additional studies, the data indicate that ASIC3 and PSD-95 are both present in the spinal cord and DRG where they might interact. The presence of transcripts for Lin-7b, MAGI-1b, and PIST suggest that they might also be present at the same site as ASIC3.

To test for an interaction between ASIC3 and PSD-95 *in vivo*, we immunoprecipitated PSD-95 from spinal cord and found

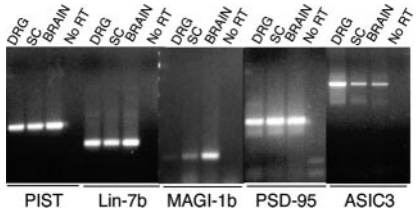

FIG. 5. **Transcripts for ASIC3, PSD-95, MAGI-1b, Lin-7b, and PIST are found in brain, spinal cord (*SC*), and DRG.** RT-PCRs for the indicated mRNAs were performed using mouse brain, spinal cord, and dorsal root ganglion. Shown is an ethidium bromide-stained agarose gel.

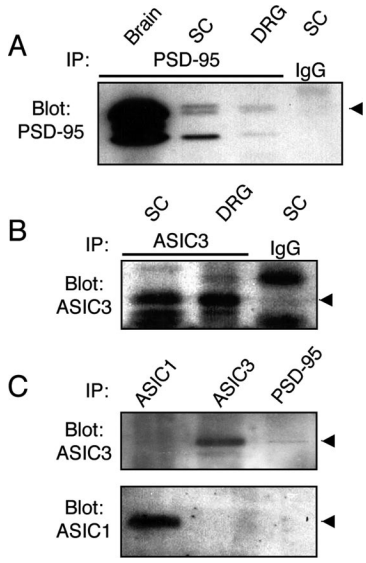

FIG. 6. **PSD-95 co-immunoprecipitates ASIC3 from spinal cord.** *A* and *B*, tissue lysates (500 μg) from brain, spinal cord, and dorsal root ganglia were immunoprecipitated and blotted for PSD-95 (*A*) or ASIC3 (*B*). Rabbit IgG was used as a control for the immunoprecipitations. PSD-95 appeared as more than one band as reported previously (47). *C*, tissue lysates from spinal cord (500 μg) were immunoprecipitated with anti-PSD-95, anti-ASIC3, or anti-ASIC1 antibodies. Immunoblots were with anti-ASIC3 and anti-ASIC1 antibodies. $n = 3$. *IP*, immunoprecipitation; *SC*, spinal cord.

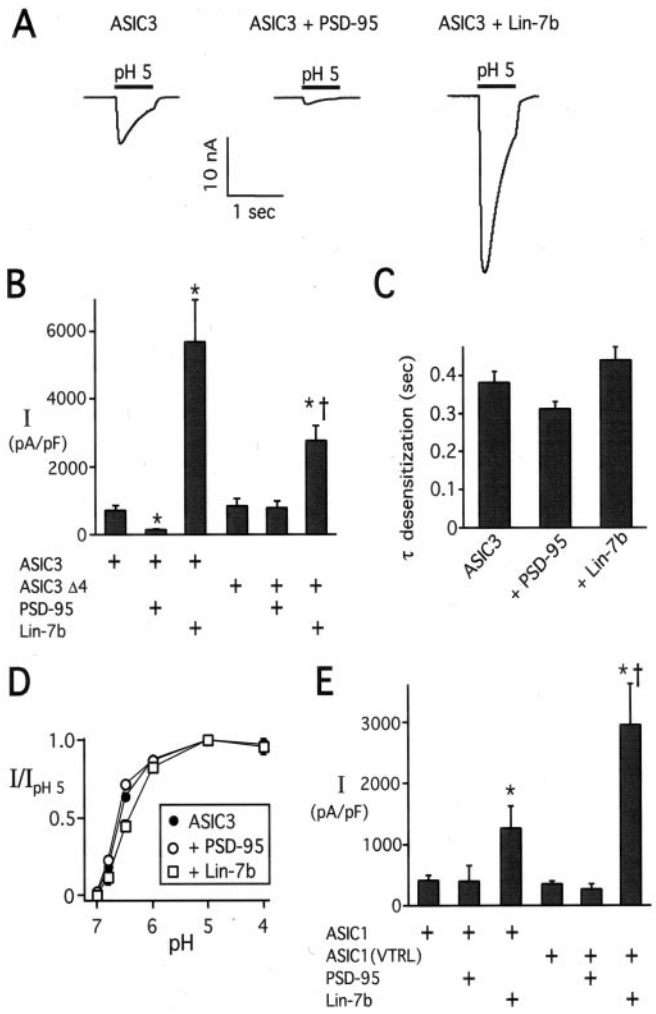

FIG. 7. **PDZ proteins alter ASIC3 acid-evoked current.** *A*, representative H^+-gated currents in CHO cells expressing ASIC3 alone or with the indicated constructs. The solution was changed from pH 7.4 to 5 during the time indicated by the *bar*. The ratio of cDNA for ASIC3 to PSD-95, Myc-Lin-7b, or dsRed (used as a control in all studies) was 1:10. *B*, peak current densities evoked by pH 5 application to CHO cells expressing the indicated constructs. Data are mean ± S.E.; $n = 8$–39. *, $p < 0.01$ compared with ASIC3;†, $p < 0.05$ compared with ASIC3 + Lin-7b. *C*, time constants of desensitization as measured from single exponential fits to the falling phase of the currents evoked by pH 6 application. $n = 8$–16. *D*, relationship between pH and current. Currents were normalized to those evoked by pH 5. $n \geq 9$ cells for all points. *E*, peak current densities evoked by pH 5 application to CHO cells coexpressing ASIC1a or ASIC1a with the terminal 4 amino acids mutated to VTRL ($ASIC1_{VTRL}$) with either PSD-95 or Lin-7b. $n = 8$–16; *, $p \leq 0.05$ compared with ASIC1; †, $p < 0.05$ compared with ASIC1 + Lin-7b. *pF*, picofarads.

that it co-precipitated ASIC3 (Fig. 6*C*). In contrast, PSD-95 did not co-precipitate with ASIC1, which is also expressed in spinal cord (38).

PSD-95 and Lin-7b Alter ASIC3 H^+-gated Currents—The interaction of these proteins with ASIC3 suggested they might alter its current. Application of a pH 5 solution to CHO cells expressing ASIC3 generated transient inward currents (Fig. 7*A*), consistent with previous reports (1, 2). Coexpression of rat ASIC3 with PSD-95 reduced the amplitude of acid-evoked currents ~5-fold (Fig. 7, *A* and *B*). When we coexpressed ASIC3 with Lin-7b, we obtained the opposite result, current density increased ~8-fold. The PSD-95- and Lin-7b-induced alterations in current amplitude occurred without major changes in the rate of current desensitization or the sensitivity to pH (Fig. 7, *C* and *D*). Both MAGI-1b and PIST altered current with an increase of ~2.5- and ~2.1-fold increase over control, respectively, with no change in channel properties. Because PSD-95 and Lin-7b had the largest and opposite effects on ASIC3 current, we studied their effects on ASIC3 in more detail.

To learn whether the functional effects arose from an interaction of the ASIC3 PDZ-binding motif with PSD-95 and Lin-7b, we repeated the experiments with rat ASIC3 missing its 4 C-terminal residues (ASIC3Δ4). When expressed alone, ASIC3 and ASIC3Δ4 generated H^+-gated currents of similar amplitude, but without the C-terminal residues the effects of PSD-95 and Lin-7b were blunted (Fig. 7*B*).

The results indicate that the PDZ-binding motif of ASIC3 is required for the interaction with PSD-95 and Lin-7b. As an additional test of specificity, we studied ASIC1a; PSD-95 had no effect, while Lin-7b showed a small increase in current (Fig. 7*E*). To test whether the C-terminal motif of ASIC3 is sufficient for an effect on function, we substituted the 4 C-terminal amino acids of ASIC1a with those of rat ASIC3 ($ASIC1_{VTRL}$). With this C-terminal addition, Lin-7b increased acid-evoked currents (Fig. 7*E*). However, PSD-95 did not significantly reduce current generated by $ASIC1_{VTRL}$. These data indicate that PSD-95 and Lin-7b have opposite effects on ASIC3 current; PSD-95 reduces current amplitude, while Lin-7b increases it, and both effects require the ASIC3 PDZ-binding motif.

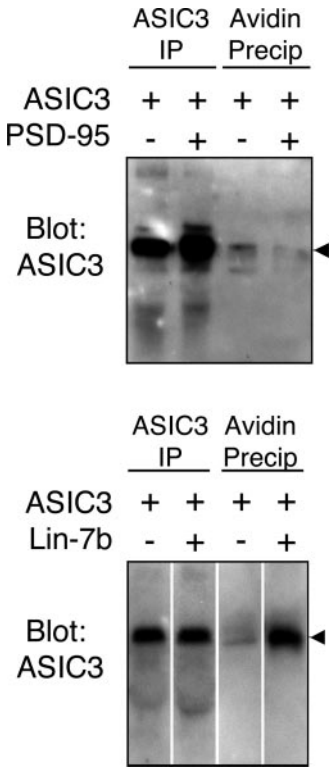

FIG. 8. **PSD-95 decreases and Lin-7b increases ASIC3 on the cell surface.** COS-7 cells were cotransfected with ASIC3 and PSD-95-GFP, Myc-Lin-7b, or empty vector. Two days later, cell surface proteins were biotinylated at 4 °C. 500 μg of cell lysate was used to isolate labeled surface proteins using neutravidin beads or ASIC3 by immunoprecipitation with anti-ASIC3 antibodies. Blots were with anti-ASIC3 antibody. *Lanes* in the *bottom* blot were all from the same gel and film exposure but were arranged for the purpose of illustration. Experiments were performed five times with PSD-95 and twice with Lin-7b, each obtaining similar results. *IP*, immunoprecipitation; *Precip*, precipitation.

PSD-95 Decreases and Lin-7b Increases ASIC3 Surface Expression—Because PSD-95 and Lin-7b altered current density but did not change the properties of ASIC3 H^+-gated currents, we hypothesized that these adapter proteins might change the amount of ASIC3 on the cell surface. To test this hypothesis, we used biotinylation to label ASIC3 that was present on the cell surface (Fig. 8). We found that PSD-95 reduced and Lin-7b increased the amount of labeled ASIC3. These data suggest that PSD-95 and Lin-7b alter current by controlling the amount of ASIC3 on the cell surface.

DISCUSSION

Our results demonstrate that ASIC3 binds the PDZ domain-containing proteins PSD-95, Lin-7b, MAGI-1b, and PIST. These interactions occurred through a PDZ-binding motif at the C terminus of ASIC3 as shown by the yeast two-hybrid assay and co-immunoprecipitation in COS-7 cells. In addition, for some of the interactions, coexpression altered the pattern of immunostaining in COS-7 cells. Moreover we found that PSD-95 coimmunoprecipitated ASIC3 from spinal cord. However, the interactions differed for the various PDZ-containing proteins; the most striking difference occurred when ASIC3 was coexpressed with PSD-95 and Lin-7b.

PSD-95 reduced ASIC3 acid-evoked currents. Current fell because PSD-95 decreased the amount of ASIC3 in the cell membrane. ASIC3 currents measured in the presence of PSD-95 retained the acid sensitivity and desensitization rate of ASIC3 expressed alone, consistent with a reduction in the number of cell surface channels rather than an alteration of their properties. The finding that PSD-95 did not reduce the total amount of ASIC3 in the cell suggested that it did not decrease cell surface protein by stimulating ASIC3 degradation. Although Lin-7b also bound the C terminus of ASIC3, it had an effect opposite from that of PSD-95. Lin-7b increased ASIC3 current by increasing ASIC3 cell surface expression. Like PSD-95, we found no evidence that the interaction altered the properties of ASIC3 currents. Consistent with our findings, recent studies have shown that Lin-7b interacted with and retained the epithelial γ-aminobutyric acid transporter (BGT-1) at the membrane of Madin-Darby canine kidney cells (39). Lin-7b also stabilized the inward rectifying K^+ channel Kir 2.3 at the plasma membrane, thereby increasing channel current (40). The functional expression of *Xenopus* ENaC, a member of the DEG/ENaC family, also requires its association with Apx (apical protein *Xenopus*) and α-spectrin, which may sequester and stabilize ENaC at the cell surface (41). Interactions with more than one protein containing a PDZ domain have also been observed to regulate CFTR; PIST (CAL) reduces and the Na^+/H^+ exchanger-regulatory factor increases CFTR expression on the cell surface (28). A recent report indicated that CIPP also increased ASIC3 currents (18). Although the mechanism was not investigated, like Lin-7b, CIPP did not alter the properties of ASIC3 currents. Thus, we speculate that as with Lin-7b, CIPP may also increase the amount of ASIC3 in the plasma membrane.

Although we found that four different proteins (PSD-95, Lin-7b, MAGI-1b, and PIST) interacted with the ASIC3 C terminus, there were differences. For example, in the yeast two-hybrid assay the Arg at position -1 in ASIC3 was important for the interaction with PIST but not MAGI-1b or Lin-7b. In addition, while the ASIC3 PDZ-binding motif was required for the functional effects of both Lin-7b and PSD-95, incorporating the ASIC3 C terminus on ASIC1a reconstituted the stimulatory effect of Lin-7b but not the current reduction produced by PSD-95. Thus additional sequences in ASIC3 appear to be necessary for PSD-95 to interact with ASIC3; similar conclusions have been made for the interaction between other PDZ domain proteins and their partners (42, 43).

The findings suggest the possibility of substantial complexity in the interactions of ASIC3 with a cytoplasmic scaffold built from multiple components. Although we show an *in vivo* interaction with PSD-95, ASIC3 may interact with some or all of the other proteins identified here as well as with CIPP (18). As with other DEG/ENaC channels (10, 44), several ASIC subunits multimerize to form a functional channel, providing a single channel complex with the opportunity for multiple interactions. Conversely several of the interacting proteins have more than one PDZ domain (MAGI-1b has five, CIPP has four, and PSD-95 has three), suggesting they could bind more than one of the C termini in an ASIC3 channel or other receptors and channels at the same time. In addition, because ASIC3 heteromultimerizes with other ASIC subunits, ASIC3 might be drawn indirectly into interactions with other proteins such as PICK1, which binds ASIC1 and ASIC2 (14, 15). Moreover the PDZ-containing proteins we identified could generate additional interactions because they also contain other protein-binding domains, including leucine zipper, Src homology 3, WW, guanylate kinase, and coiled-coil domains.

In addition to its previously demonstrated importance in peripheral neurons, our data identify ASIC3 in the spinal cord where it interacts with PSD-95. Interestingly spinal cord PSD-95 also interacts with the *N*-methyl-D-aspartate receptor NR2A/B (37); both ASIC3 and NR2 subunits also bind Lin-7b and MAGI-2 (26, 31, 36). The presence of ASIC3, NR2 subunits, and this scaffolding complex in the spinal cord raises questions about

ASIC3 function at that site. Recent studies in PSD-95 mutant mice and mice injected with PSD-95 antisense oligonucleotides have shown a reduction in the neuropathic reflex sensitization that develops upon thermal and mechanical hyperalgesia (37, 45, 46). In addition, mice lacking ASIC3 failed to develop mechanical hyperalgesia and central sensitization that normally follow repeated intramuscular acid (5). Our data combined with earlier studies suggest that this sensitization might be due to signaling mechanisms in either peripheral or spinal cord neurons. In either case, they suggest that ASIC3 may be a target for the development of agents targeting nociception.

These findings suggest that ASIC3 interacts with a complex intracellular protein scaffold. These interactions could influence channel function in a number of ways. They might modulate nociceptive and mechanosensory functions by controlling the amount of cell surface protein and hence total ASIC3 current. They might also influence ASIC3 localization. Because the contribution of DEG/ENaC channels, including ASIC3, to mechanosensation may involve a tethered channel mechanism, interactions with an intracellular scaffold may also be a key component of the mechanosensory process.

Acknowledgments—We thank Pary Weber, Tamara Nesselhauf, Matthew J. Thoendel, Amin M. Nekoomand, Robert J. Thompson, Kate M. Cooper, Kerry E. Wilkins, Jillian M. Henss, Jayasheel O. Eshcol, Philip Karp, and Theresa A. Mayhew for excellent assistance. We thank the University of Iowa DNA Core Facility for assistance with sequencing and oligonucleotide synthesis. We thank the *In Vitro* Models and Cell Culture Core for preparing cells.

REFERENCES

1. Waldmann, R., Bassilana, F., de Weille, J. R., Champigny, G., Heurteaux, C., and Lazdunski, M. (1997) *J. Biol. Chem.* **272,** 20975–20978
2. Babinski, K., Le, K. T., and Séguéla, P. (1999) *J. Neurochem.* **72,** 51–57
3. Price, M. P., McIllwrath, S. L., Xie, J., Cheng, C., Qiao, J., Tarr, D. E., Sluka, K. A., Brennan, T. J., Lewin, G. R., and Welsh, M. J. (2001) *Neuron* **32,** 1071–1083
4. Chen, C. C., Zimmer, A., Sun, W. H., Hall, J., and Brownstein, M. J. (2002) *Proc. Natl. Acad. Sci. U. S. A.* **99,** 8992–8997
5. Sluka, K. A., Price, M. P., Breese, N. M., Stucky, C. L., Wemmie, J. A., and Welsh, M. J. (2003) *Pain* **106,** 229–239
6. Benson, C. J., Eckert, S. P., and McCleskey, E. W. (1999) *Circ. Res.* **84,** 921–928
7. Sutherland, S. P., Benson, C. J., Adelman, J. P., and McCleskey, E. W. (2001) *Proc. Natl. Acad. Sci. U. S. A.* **98,** 711–716
8. Xie, J., Price, M. P., Berger, A. L., and Welsh, M. J. (2002) *J. Neurophysiol.* **87,** 2835–2843
9. Alvarez de la Rosa, D., Zhang, P., Shao, D., White, F., and Canessa, C. M. (2002) *Proc. Natl. Acad. Sci. U. S. A.* **99,** 2326–2331
10. Benson, C. J., Xie, J., Wemmie, J. A., Price, M. P., Henss, J. M., Welsh, M. J., and Snyder, P. M. (2002) *Proc. Natl. Acad. Sci. U. S. A.* **99,** 2338–2343
11. Mano, I., and Driscoll, M. (1999) *Bioessays* **21,** 568–578
12. Benos, D. J., and Stanton, B. A. (1999) *J. Physiol.* (*Lond*). **520,** 631–644
13. Welsh, M. J., Price, M. P., and Xie, J. (2002) *J. Biol. Chem.* **277,** 2369–2372
14. Hruska-Hageman, A. M., Wemmie, J. A., Price, M. P., and Welsh, M. J. (2002) *Biochem. J.* **361,** 443–450
15. Duggan, A., Garcia-Anoveros, J., and Corey, D. P. (2002) *J. Biol. Chem.* **277,** 5203–5208
16. Baron, A., Deval, E., Salinas, M., Lingueglia, E., Voilley, N., and Lazdunski, M. (2002) *J. Biol. Chem.* **277,** 50463–50468
17. Leonard, A. S., Yermolaieva, O., Hruska-Hageman, A., Askwith, C. C., Price, M. P., Wemmie, J. A., and Welsh, M. J. (2003) *Proc. Natl. Acad. Sci. U. S. A.* **100,** 2029–2034
18. Anzai, N., Deval, E., Schaefer, L., Friend, V., Lazdunski, M., and Lingueglia, E. (2002) *J. Biol. Chem.* **277,** 16655–16661
19. Wemmie, J. A., Chen, J., Askwith, C. C., Hruska-Hageman, A. M., Price, M. P., Nolan, B. C., Yoder, P. G., Lamani, E., Hoshi, T., Freeman, J. H., Jr., and Welsh, M. J. (2002) *Neuron* **34,** 463–477
20. Adams, C. M., Snyder, P. M., and Welsh, M. J. (1997) *J. Biol. Chem.* **272,** 27295–27300
21. Leonard, A. S., and Hell, J. W. (1997) *J. Biol. Chem.* **272,** 12107–12115
22. Dobrosotskaya, I., Guy, R. K., and James, G. L. (1997) *J. Biol. Chem.* **272,** 31589–31597
23. Laura, R. P., Ross, S., Koeppen, H., and Lasky, L. A. (2002) *Exp. Cell Res.* **275,** 155–170
24. Borg, J. P., Straight, S. W., Kaech, S. M., de Taddeo-Borg, M., Kroon, D. E., Karnak, D., Turner, R. S., Kim, S. K., and Margolis, B. (1998) *J. Biol. Chem.* **273,** 31633–31636
25. Butz, S., Okamoto, M., and Sudhof, T. C. (1998) *Cell* **94,** 773–782
26. Jo, K., Derin, R., Li, M., and Bredt, D. S. (1999) *J. Neurosci.* **19,** 4189–4199
27. Neudauer, C. L., Joberty, G., and Macara, I. G. (2001) *Biochem. Biophys. Res. Commun.* **280,** 541–547
28. Cheng, J., Moyer, B. D., Milewski, M., Loffing, J., Ikeda, M., Mickle, J. E., Cutting, G. R., Li, M., Stanton, B. A., and Guggino, W. B. (2002) *J. Biol. Chem.* **277,** 3520–3529
29. Charest, A., Lane, K., McMahon, K., and Housman, D. E. (2001) *J. Biol. Chem.* **276,** 29456–29465
30. Songyang, Z., Fanning, A. S., Fu, C., Xu, J., Marfatia, S. M., Chishti, A. H., Crompton, A., Chan, A. C., Anderson, J. M., and Cantley, L. C. (1997) *Science* **275,** 73–77
31. Hirao, K., Hata, Y., Ide, N., Takeuchi, M., Irie, M., Yao, I., Deguchi, M., Toyoda, A., Sudhof, T. C., and Takai, Y. (1998) *J. Biol. Chem.* **273,** 21105–21110
32. Kornau, H. C., Schenker, L. T., Kennedy, M. B., and Seeburg, P. H. (1995) *Science* **269,** 1737–1740
33. Cho, K. O., Hunt, C. A., and Kennedy, M. B. (1992) *Neuron* **9,** 929–942
34. Kim, E., Niethammer, M., Rothschild, A., Jan, Y. N., and Sheng, M. (1995) *Nature* **378,** 85–88
35. Irie, M., Hata, Y., Takeuchi, M., Ichtchenko, K., Toyoda, A., Hirao, K., Takai, Y., Rosahl, T. W., and Sudhof, T. C. (1997) *Science* **277,** 1511–1515
36. Hirao, K., Hata, Y., Yao, I., Deguchi, M., Kawabe, H., Mizoguchi, A., and Takai, Y. (2000) *J. Biol. Chem.* **275,** 2966–2972
37. Tao, Y. X., Huang, Y. Z., Mei, L., and Johns, R. A. (2000) *Neuroscience* **98,** 201–206
38. Alvarez de la Rosa, D., Krueger, S. R., Kolar, A., Shao, D., Fitzsimonds, R. M., and Canessa, C. M. (2003) *J. Physiol.* (*Lond.*) **546,** 77–87
39. Perego, C., Vanoni, C., Villa, A., Longhi, R., Kaech, S. M., Frohli, E., Hajnal, A., Kim, S. K., and Pietrini, G. (1999) *EMBO J.* **18,** 2384–2393
40. Olsen, O., Liu, H., Wade, J. B., Merot, J., and Welling, P. A. (2002) *Am. J. Physiol.* **282,** C183–C195
41. Zuckerman, J. B., Chen, X., Jacobs, J. D., Hu, B., Kleyman, T. R., and Smith, P. R. (1999) *J. Biol. Chem.* **274,** 23286–23295
42. Lim, I. A., Hall, D. D., and Hell, J. W. (2002) *J. Biol. Chem.* **277,** 21697–21711
43. Hanley, J. G., Khatri, L., Hanson, P. I., and Ziff, E. B. (2002) *Neuron* **34,** 53–67
44. Kosari, F., Berdiev, B. K., Li, J., Sheng, S., Ismailov, I., and Kleyman, T. R. (1999) in *Current Topics in Membranes, The Physiology and Functional Diversity of Amiloride-Sensitive Na^+ Channels: A New Gene Superfamily* (Benos, D., ed) Vol. 47, pp. 37–48, Academic Press, San Diego, CA
45. Garry, E. M., Moss, A., Delaney, A., O'Neill, F., Blakemore, J., Bowen, J., Husi, H., Mitchell, R., Grant, S. G., and Fleetwood-Walker, S. M. (2003) *Curr. Biol.* **13,** 321–328
46. Tao, F., Tao, Y. X., Mao, P., and Johns, R. A. (2003) *Neuroscience* **117,** 731–739
47. Sans, N., Petralia, R. S., Wang, Y. X., Blahos, J., II, Hell, J. W., and Wenthold, R. J. (2000) *J. Neurosci.* **20,** 1260–1271